

Provided for non-commercial research and education use.
Not for reproduction, distribution or commercial use.



This article appeared in a journal published by Elsevier. The attached copy is furnished to the author for internal non-commercial research and education use, including for instruction at the authors institution and sharing with colleagues.

Other uses, including reproduction and distribution, or selling or licensing copies, or posting to personal, institutional or third party websites are prohibited.

In most cases authors are permitted to post their version of the article (e.g. in Word or Tex form) to their personal website or institutional repository. Authors requiring further information regarding Elsevier's archiving and manuscript policies are encouraged to visit:

<http://www.elsevier.com/copyright>

available at www.sciencedirect.comjournal homepage: www.ejconline.com

New insights of mitochondria reactive oxygen species generation and cell apoptosis induced by low dose photodynamic therapy

Hongyou Zhao ^a, Da Xing ^{a,b,*}, Qun Chen ^a

^a MOE Key Laboratory of Laser Life Science and Institute of Laser Life Science, College of Biophotonics, South China Normal University, Guangzhou 510631, China

^b Joint Laboratory of Laser Oncology with Cancer Center of Sun Yat-sen University, South China Normal University, Guangzhou 510631, China

ARTICLE INFO

Article history:

Available online 6 July 2011

Keywords:

Low dose PDT
Mitochondria
Respiration-deficient cell
Endogenous ROS
Apoptosis

ABSTRACT

Photodynamic therapy (PDT) is an approved therapeutic procedure that exerts cytotoxic activity towards tumour cells by irradiating photosensitisers with light exposure to produce reactive oxygen species (ROS). In the current study, we have observed that there is an additional production of intracellular ROS during low dose PDT. A mitochondrial respiration-deficient cell line (ρ^0 cells) was investigated to determine the involvement of electron transfer chain (ETC). The production of ROS was significantly different between ASTC-a-1 and ρ^0 ASTC-a-1 cells after an identical PDT treatment. Yet, with an increasing Photofrin dose, the difference gradually diminished. Pretreatment of the ASTC-a-1 cells with the ETC inhibitor rotenone lead the corresponding ROS production to a similar level from ρ^0 ASTC-a-1 cells subjected to identical PDT protocols. Moreover, we found that the difference in intracellular ROS productions between ASTC-a-1 and ρ^0 ASTC-a-1 cells started during a PDT treatment, while the irradiation was still being delivered. A cytotoxicity assay showed that, the ASTC-a-1 cells were more sensitive to PDT than ρ^0 ASTC-a-1 cells. ROS scavenger *n*-acetyl-l-cysteine (NAC) attenuated the toxicity of PDT in both cell lines. Altogether, these results indicate that low dose PDT can induce an endogenous ROS production via the ETC. This additional endogenous ROS, on top of that from PDT photochemical reactions, contributes to an increased cell apoptosis. Thus, mitochondria are not only targets but also can be a source of ROS during low dose PDT. These results may provide a novel approach to improve PDT applications by maximising the efficiency of currently available photosensitisers.

© 2011 Elsevier Ltd. All rights reserved.

1. Introduction

Photodynamic therapy utilises an exogenously administered photosensitiser activated by light energy to achieve a localised cytotoxicity for treatment of various indications.¹ Its re-

cent development focuses on not only new photosensitisers, but also optimising treatment protocols for the existing drugs to maximise their efficiency. In contrast to that in a conventional photodynamic therapy (PDT) treatment that typically lasts less than an hour, prolonged, low-irradiance light

* Correspondence author: Address: MOE Key Laboratory of Laser Life Science and Institute of Laser Life Science, College of Biophotonics, South China Normal University, Guangzhou 510631, China. Tel.: +86 20 85210089; fax: +86 20 85216052.

E-mail address: xingda@scnu.edu.cn (D. Xing).

0959-8049/\$ - see front matter © 2011 Elsevier Ltd. All rights reserved.

doi:10.1016/j.ejca.2011.06.031

delivery has been reported to be more effective to eradicate tumour. The mechanism for the phenomenon has been interpreted primarily as a combination of improved tissue re-oxygenation and reduced effects by oxygen bleaching.^{2,3} Indeed, the presence of molecular oxygen is critical for PDT because the cytotoxic agent, singlet oxygen ($^1\text{O}_2$), arises as a result of the energy transfer from the excited photosensitizer to ground state oxygen ($^3\text{O}_2$) residing in the target tissue.^{4,5} It is well established that low-fluence rate PDT allows the tissue additional time to obtain oxygen from the vasculature.

Many reports have implicated mitochondria as important targets of PDT. Photosensitisers that localise to mitochondria are reported to be more efficient in killing cells than those localise at other cellular sites.^{6,7} This is evident for the most commonly used photosensitiser Photofrin. It has been proposed that the initial response to Photofrin mediated PDT is a formation of azidesensitive $^1\text{O}_2$ in mitochondria. Subsequently, this mitochondrial reactive oxygen species (ROS) induces mitochondrial inner membrane permeabilisation resulting in mitochondrial depolarisation, swelling, cytochrome *c* release and the subsequent apoptotic death.^{8,9} It is also reported that a blockade of mitochondrial ROS production can protect against PDT-induced apoptotic death.¹⁰ Overall, these studies have shown that mitochondrial ROS plays a critical role in PDT-induced apoptosis.

There are other factors to be considered too. The mitochondrial electron-transport chain is the main source of ROS during normal cellular metabolism.^{11,12} The rate of ROS production from electron transfer chain (ETC) can increase under a variety of pathologic conditions including hyperoxia,^{13,14} photostimulation,¹⁵ oxygen reperfusion,¹⁶ aging,¹⁷ and chemical inhibition of mitochondrial respiration.^{18,19} Mitochondria contain some 1000 proteins that are encoded in the nuclear DNA and are imported after synthesis on cytoplasmic ribosomes; only 13 proteins are encoded by mitochondrial DNA, including 7 of NADH-Q reductase, 1 of cytochrome *c* reductase, 3 of cytochrome *c* oxidase and 2 of ATP synthase.²⁰ Therefore, in ρ^0 cells that lack mtDNA, respiratory chain is considered practically non-functioning.^{21,22} The ETC will not have an increase in production of ROS under extraneous stresses.^{23–25}

The results from the present study not only support the concept that mitochondria is a target of PDT oxidative damage, but also demonstrate that mitochondria itself can be a source of ROS during at least Photofrin mediated PDT. The establishment of ASTC-a-1 cell line lacking mitochondrial DNA enabled us to conduct real-time imaging of ROS production at single cell level without ROS generated by the ETC during PDT. More importantly, with the results obtained with the cell model, we have demonstrated that ROS generated by the ETC contribute to increased apoptosis during low dose PDT.

2. Materials and methods

2.1. Cell culture

The human lung adenocarcinoma cell line (ASTC-a-1) was obtained from the Department of Medicine (Jinan University, Guangzhou, Guangdong, People's Republic of China). Cells were cultured in dulbecco's modified eagle medium (DMEM)

supplemented with 15% foetal calf serum, penicillin (100 U/ml) and streptomycin (100 mg/ml) in 5% CO_2 at 37 °C in a humidified incubator. Respiration-deficient ASTC-a-1 cells (ρ^0 cells) were generated by incubating wild-type cells in ethidium bromide for 4 week in medium supplemented with pyruvate and uridine.²⁶ The ρ^0 cells were then selected by exposure of the mitochondrial inhibitors rotenone (1 $\mu\text{g}/\text{ml}$) and antimycin A (1 $\mu\text{g}/\text{ml}$), which are lethal to wild-type cells. Cells were considered ρ^0 cells when there was no detectable cytochrome *b* by polymerase chain reaction (PCR).²⁴

2.2. Reagents

Photofrin (Sinclair Pharmaceuticals, Guildford, UK); DMEM was purchased from Invitrogen (Carlsbad, CA). Rotenone, *n*-acetyl-l-cysteine (NAC), antimycin A, pyruvate and uridine were purchased from Sigma. The following fluorophore probes were used: MitoTracker Red (100 nM, Invitrogen Life Technologies, Inc.) to label mitochondria. 2',7'-dichlorodihydrofluorescein diacetate (2',7'-dichlorodihydrofluorescein diacetate (H_2DCFDA), 10 μM , Molecular Probes, Inc.) to detect the generation of ROS. Staurosporine was purchased from PeProTech (Rocky Hill, NJ).

2.3. Photodynamic therapy

The PDT irradiation light source was a He-Ne laser (HN-1000, Guangzhou, China; 632.8 nm). Cells (1×10^5 per well) growing in 35 mm Petri dishes were co-incubated with Photofrin in complete growth medium in the dark. After 18 h of incubation, the cells were rinsed with phosphate-buffered saline (PBS). The long incubation period was used to ensure the mitochondrial localisation of Photofrin. For the following experiments, cells were irradiated at 3 mW/cm^2 . For the control group, cells were incubated in the same medium without Photofrin or light.

2.4. Imaging analysis of living cells

In order to image the activities of a single cell, a confocal laser scanning microscope system was used. Fluorescent emissions from H_2DCFDA (DCF), Photofrin and MitoTracker Red were monitored confocally using a commercial laser scanning microscope (LSM 510 Meta) combination system (Carl Zeiss, Jena, Germany) equipped with a Plan-Neofluar 40 \times /1.3 numerical aperture (NA) oil differential interference contrast (DIC) objective. Excitation wavelength and detection filter settings for each of the fluorescent indicators were as follows: DCF fluorescence was excited at 488 nm with an Ar-Ion laser, and the emission was recorded through a 500 to 550 nm band pass filter. Photofrin fluorescence was excited at 458 nm with an Ar-Ion laser, and emitted light was recorded through a 600–650 nm band-pass filter. MitoTracker Red fluorescence was excited at 633 nm with a He-Ne laser, and the emitted signal was recorded through a 650 nm long-pass filter. For intracellular measurements, a desired measurement position was chosen in the LSM image. To quantify the results, the emission intensities were processed with Laser Scanning Microscope LSM510/Confocor 2 Version 3.2 SP2 (Zeiss, Germany).

2.5. Measurement of intracellular ROS

Cellular ROS generation was assayed with DCF. ASTC-a-1 and ρ^0 ASTC-a-1 cells were incubated with 10 μ M DCF at 37 °C for 30 min prior to the harvest time point. The cells were then washed, exposed to light, re-suspended in FACS buffer (PBS1%FBS) and analysed by flow cytometry using a FACSort flow cytometer (BD Biosciences, San Diego, CA). Excitation was set at 488 nm, and emission was recorded on an FL1 detector (525 nm). Electronic compensation was used to eliminate spreading into adjacent fluorescence channels. The data were analysed with CellQuest™ software (BD Biosciences, San Diego, CA, USA).

2.6. Photosensitiser uptake

To determine whether a difference in intracellular photosensitiser concentration could be responsible for a potential discrepancy in PDT sensitivity between ASTC-a-1 and ρ^0 ASTC-a-1 cells, total levels of photosensitisers in the cells were measured with absorbance spectroscopy (Perkin-Elmer, USA). The excitation wavelength was 395 nm, the emission wavelength was 633 nm. Cells were cultured in a 12-well microplate at a density of 1×10^5 cells per well for 24 h and then co-incubated with various concentrations of Photofrin for 18 h at 37 °C in the dark. Cells were harvested, washed briefly with Dulbecco's phosphate-buffered saline (DPBS) and resuspended in DPBS. An aliquot was retained from each sample for protein assay (Biorad method). The photosensitiser was then extracted from the cell pellets with methanol by vigorous vortex mixing, and the absorbance read at the spectral peak against a blank of extracted cells without added photosensitiser.²⁷

2.7. Lactate production, glucose uptake and intracellular ATP content

To determine the cellular lactate production, cells in exponential growth phase were washed and incubated with fresh medium for the indicated times. Aliquots of the culture medium were removed for the analysis of lactate content using an Accutrend lactate analyser with a linear range of standard lactate concentrations according to the procedures recommended by the manufacturer (Roche, Mannheim, Germany). Cellular glucose uptake was measured by incubating cells in glucose-free DMEM with 0.2 Ci/mL [³H] 2-deoxyglucose (specific activity, 40 Ci/mmol) for 60 min. After the cells were washed with ice-cold PBS, the radioactivity in the cell pellets was quantified by liquid scintillation counting. The intracellular ATP content was measured with ATP Determination Kit (Sigma).

2.8. Annexin flow cytometry

For flow cytometric analysis (FACS analysis), Annexin-V-FITC conjugate and binding buffer were used as standard reagents. Flow cytometry was performed on a FACScanto flow cytometer (Becton Dickinson, Mountain View, CA) with excitation at 488 nm. Fluorescent emission of FITC was measured at 515–545 nm and that of DNA-PI complexes at 564–606 nm.

Cell debris was excluded from analysis by an appropriate forward light scatter threshold setting. Compensation was used wherever necessary.

2.9. Polymerase chain reaction (PCR)

FlexGen DNA Kit (Cwbio) was used to isolate total cellular DNA from ASTC-a-1 and ρ^0 ASTC-a-1 cells. The primers were designed according to the sequences of GenBank. Thermal cycling conditions involved 45 cycles, with denaturation at 95 °C for 30 s, annealing at 55 °C for 30 s and extension at 72 °C for 30 s, using 0.5 μ mol/L of intron-spanning primers. Five microlitres of the PCR were electrophoresed on a 1% agarose gel. The primers used for PCR were as follows: cytochrome *b*, forward: 5'-ATAAACATTACTCTGGTCTTGTAAC-3' and reverse: 5'-ATTAATTTAAAGGCCAGGACCAAACCT-3', β -actin, forward: 5'-GAGCTACGAGCTGCCTGACG-3' and reverse: 5'-CCTAGAAGCATTTGCGGTGG-3'.

2.10. Mitochondrial isolation

For mitochondria isolation, cells were harvested and then fractionated using Cytosol/Mitochondria Fractionation Kit (Merch, Germany) according to the supplier's recommendations. The cytosol extraction and mitochondria were then subjected to western blotting analysis of cytochrome *c*, respectively. The purity of fractions was tested by immunoblotting with antibodies specific for the cytosolic proteins β -actin or the mitochondrial proteins VCDA1/Porin.

2.11. Antibodies and Western blotting analysis

The antibodies used for Western blotting include antibodies against caspase-3 (full), caspase-3 (cleaved), cytochrome *c* (Cell Signaling Technology, Danvers, MA). At indicated times after PDT, cells were harvested and washed twice with ice-cold PBS (pH7.4), and lysed with an ice-cold lysis buffer (50 mM Tris-HCl, pH 8.0, 150 mM NaCl, 1% Triton X-100, and 100 μ g/ml phenylmethylsulfonyl fluoride) for 30 min on ice. The lysates were centrifuged at 12,000g for 5 min at 4 °C, and the protein concentration was determined. Equivalent samples (30 μ g of protein extract was loaded on each lane) were fractionated by 12–15% SDS-PAGE. The proteins were then transferred onto a PDVF membrane (Perkin-Elmer) and probed with the indicated antibody, followed by IRDye 800 secondary antibody (Rockland Immunochemicals, Gilbertsville, PA). Detection was performed using the odyssey infra-red imaging system (LI-COR, Lincoln, NE). Equal loading was confirmed with primary antibodies against β -actin (whole-cell lysates) or VCDA1/Porin (mitochondrial preparations).

2.12. Statistics analysis

All assays were repeated independently for a minimum of three times. Data represent the mean \pm SEM. Statistical analysis was performed with Student's paired *t*-test. Differences were considered statistically significant at $P < 0.05$.

3. Results

3.1. Intracellular ROS in PDT are generated by both PDT photochemical reaction and cells themselves

Three groups of ASTC-a-1 cells were prepared. The fluorescence intensity of the intracellular photosensitizer was measured before each irradiation. ROS was measured 15 min after an irradiation. Cell death was analysed with Annexin V flow cytometry, 12 h after the irradiation. As shown in Fig. 1A, given the identical irradiation fluence, cell death was found not directly proportional to the concentration of Photofrin. There is no statistically significant difference between 2.5 and 5 µg/ml. To investigate the reason of this phenomenon, we analysed the relationships among cell death, intracellular ROS concentration and intracellular Photofrin concentration (Fig. 1B–D). The results show that the cell death is directly

proportional to the concentration of ROS, but more interestingly, we found that ROS concentration was not correlated to that of Photofrin. Specifically, for those cells treated with PDT of lower Photofrin dose (2.5 µg/ml), the total amount of intracellular ROS is more than that from direct photoactivation of Photofrin (Fig. 1D). This result clearly indicates that, ROS from direct photoactivation of Photofrin is only part of the PDT cytotoxic process, and ROS generated by cells themselves is also an important factor contributing to the overall PDT cytotoxicity.

3.2. Establishment and analysis of mitochondrial respiration-deficient cell lines (ρ^0 cells)

There are numerous sites of ROS production within cells including NAD(P)H oxidase,²⁸ xanthine oxidase²⁹ and the mitochondrial electron transport chain.^{30,31} It is well

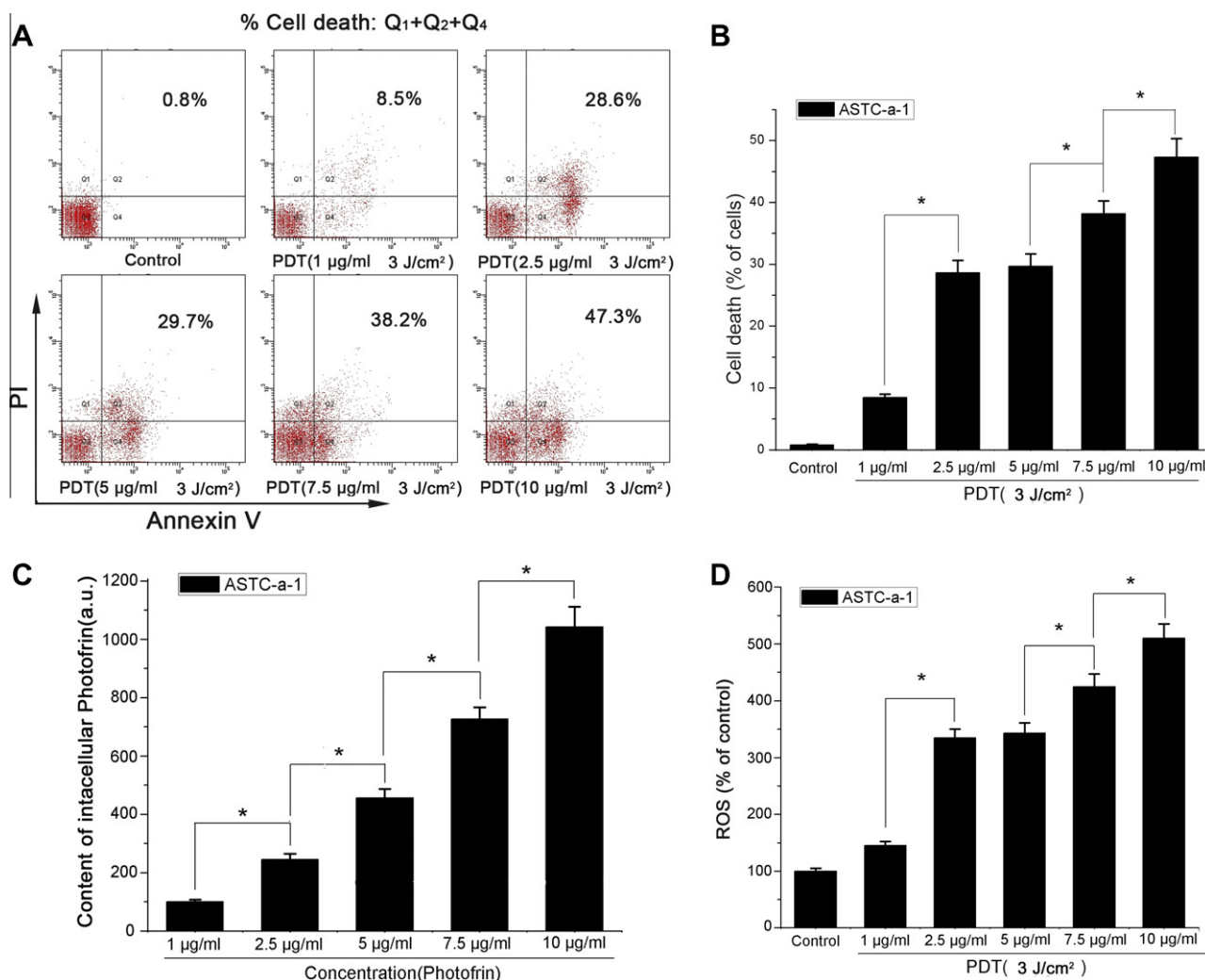


Fig. 1 – The relationships among cell death, intracellular ROS concentration and intracellular Photofrin concentration during Photofrin–PDT treatment. (A) Cell death 12 h after PDT treatment with different doses of Photofrin (1–10 µg/ml). Cells were stained with FITC-conjugated Annexin V and propidium iodide (PI). (B) Columns, mean rates of cell death expressed as the percentage of total cell number assessed by Annexin V flow cytometry. Data represent mean ± SEM (n = 3, *p < 0.05). (C) Intracellular Photofrin levels assessed by the fluorescence intensity of Photofrin, Columns, mean Photofrin fluorescence expressed as the percentage of levels measured in cells loaded with photosensitizer (2.5 µg/ml). Data represent mean ± SEM (n = 4, *p < 0.05). (D) Intracellular ROS levels assessed by DCF flow cytometry. Columns, mean DCF fluorescence expressed as the percentage of levels measured in untreated cells. Data represent mean ± SEM (n = 4, *p < 0.05).

established that Photofrin localises to mitochondria. So we conjectured that ROS generated during Photofrin mediated PDT not only leads to its own cytotoxicity, but also causes a transient burst of endogenous ROS in mitochondria. To test this conjecture, we generated respiration-deficient ASTC-a-1 cells or rho zero cells (ρ^0 cells). The absence of mitochondrial DNA was confirmed with PCR analysis of cytochrome *b* (Fig. 2A). There is no statistically significant difference between the intracellular Photofrin concentrations in the two cells, following an identical incubation protocol with Photofrin (Fig. 2B). To validate the cell line similarity, the intracellular distribution of Photofrin was investigated in two cell types. The cells were loaded with Photofrin in complete medium. Photofrin fluorescence was imaged using a laser scanning

confocal microscopy. As shown in Fig. 2C (left panel), Photofrin displayed a punctate pattern of fluorescence primarily localised to the perinuclear area. To assess whether Photofrin binds to the mitochondria, cells were co-loaded with MitoTracker, a mitochondria-specific dye. The green, punctate fluorescence shown in the Photofrin image (Fig. 2C, left panel) corresponded to MitoTracker Red fluorescence (Fig. 2C, middle panel), indicating mitochondrial localisation of Photofrin. Our results show that Photofrin localises to mitochondria in ρ^0 ASTC-a-1 cells. Compared with ASTC-a-1 cells, ρ^0 ASTC-a-1 cells were more active in glucose uptake (Fig. 2D, left columns) and produced significantly more lactate (end product of glycolytic metabolism), which was released and accumulated in the culture medium (Fig. 2D, right columns). This indicates that

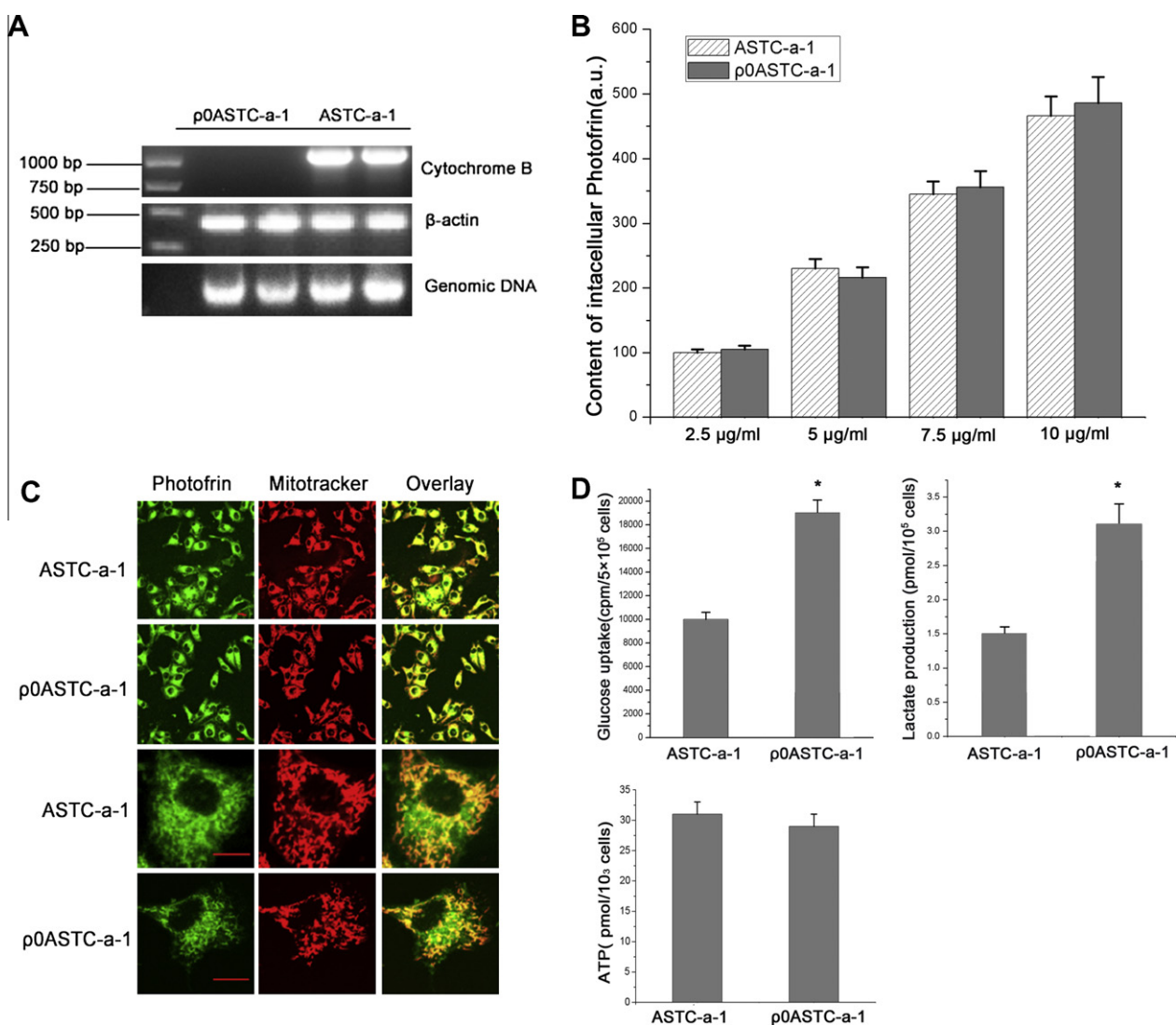


Fig. 2 – Establishment and analysis of Mitochondrial Respiration-deficient cell Lines (ρ^0 cells). (A) PCR analysis of intact ASTC-a-1 cells and rho zero (ρ^0)ASTC-a-1 cells, the latter reveals no detectable cytochrome *b*. (B) The fluorescence intensity of cell line ASTC-a-1 and ρ^0 ASTC-a-1 after incubating with various doses of photosensitiser Photofrin. Photofrin fluorescence expressed as the percentage of levels measured in ASTC-a-1 cells loaded with 2.5 μg/ml photosensitiser, data represent mean ± SEM (n = 4). (C) ASTC-a-1 and ρ^0 ASTC-a-1 cells were loaded with 10 μg/ml Photofrin and 100 nM MitoTracker Red. Photofrin fluorescence (left panel), MitoTracker Red fluorescence (middle panel) and Overlay fluorescence (right panel) were visualised by confocal microscopy. Bar = 10 μm. (D) Comparison of glucose uptake, lactate production and ATP content in ASTC-a-1 and ρ^0 ASTC-a-1 cells. Data represent mean ± SEM (n = 3, *p < 0.01).

the glycolytic pathway is highly active in these cells. Analysis of cellular ATP content (Fig. 2D, bottom columns) showed that both cells have similar cellular ATP, suggesting that the up-regulation of glycolysis was sufficient to compensate the decreased ATP generation in the mitochondria.

3.3. PDT-induced endogenous ROS are generated by the ETC of mitochondria

To determine whether endogenous ROS is related to ETC, we monitored the dynamic changes of intracellular ROS concentration in ASTC-a-1 and ρ^0 ASTC-a-1 cells during identical PDT treatment. As shown in Fig. 3A, the concentration of ROS in ASTC-a-1 cells is statistically higher than those from ρ^0 ASTC-a-1 and ASTC-a-1 cells pretreated with the rotenone. The later two were deprived of their ability to generate ETC related ROS. Compared to that in ρ^0 ASTC-a-1 cells, the ROS production in ASTC-a-1 cells proceeded in two distinct phases: the initial, slow rise due to the accumulation of ROS that from photochemical reactions (about 0–600 s), then, this primary ROS triggered the generation of endogenous ROS (after 600 s), and it reached a plateau at about 400 s after laser irradiation (Fig. 3B). The intracellular ROS concentration was measured 15 min after irradiation by FACS. Given the similarity of the two cell lines, one would expect that the quantities of ROS as a result of direct photo-excitation in the intracellular space should be at least similar during a PDT treatment. Yet, the observed total intracellular ROS concentration of ASTC-a-1 cells is significantly higher than that in the ρ^0 ASTC-a-1 cells. (Fig. 3A and C). This suggests that another source of ROS exists and the additional amount of ROS is from the mitochondria themselves. Clearly, with the mitochondria of ρ^0 ASTC-a-1 cells almost non-functional, they are not able to generate 'secondary' ROS as the normal ASTC-a-1 cells can. The inhibitor of complex I of the ETC rotenone significantly decreased the ROS concentration in ASTC-a-1 cells (Fig. 3C), while the inhibitor of NAD(P)H oxidase (diphenyliodonium) did not (results not shown). The data further confirm PDT-induced endogenous ROS are generated by ETC.

3.4. The relationship between the extent of endogenous ROS and PDT dose

The quantitative difference of the ROS concentration between the two cells gradually diminishes with the increasing of Photofrin dose (Fig. 3D). The data indicate that the extent of the PDT-induced endogenous ROS was inversely correlated with the dose of photosensitizer (from 2.5 to 10 $\mu\text{g/ml}$). The endogenous ROS reached its maximum when the Photofrin dose was 2.5 $\mu\text{g/ml}$, and it was minimal when the Photofrin dose was 10 $\mu\text{g/ml}$. The endogenous ROS significantly decreased but not disappeared, when the light dose was increased from 3 to 30 J/cm^2 with identical Photofrin dose (2.5 $\mu\text{g/ml}$) (Fig. 3E). A cytotoxicity assay showed that the maximal difference in cell killing between the two cell lines occurred at 2.5 $\mu\text{g/ml}$ of Photofrin and this difference gradually diminished as the Photofrin concentration was raised until it disappears at 10 $\mu\text{g/ml}$ (Fig. 3F, left curve). When the Photofrin dose was 2.5 $\mu\text{g/ml}$, the difference in cell killing

between the two cell lines significantly diminished but not disappeared with the increasing of light dose (Fig. 3F, right curve). When the Photofrin dose was 10 $\mu\text{g/ml}$, the difference disappeared at 3 J/cm^2 light exposure (Fig. 3G). These results demonstrate that the maximal difference in intracellular ROS and cell killing at 2.5 $\mu\text{g/ml}$ Photofrin and 3 J/cm^2 light exposure.

3.5. The cytochrome c release and caspase-3 activation in ASTC-a-1 and ρ^0 ASTC-a-1 cells after an identical PDT treatment (Photofrin 2.5 $\mu\text{g/ml}$ 3 J/cm^2)

Cytochrome c is a key apoptosis effector during apoptosis, the release of cytochrome c is an important process in PDT-induced apoptotic death. To determine whether cytochrome c is translocated into and retained within mitochondria in respiration-deficient cells, ASTC-a-1 and ρ^0 ASTC-a-1 cells were transfected with green fluorescent protein-cytochrome c (pGFP-cyt c) (green emission) and stained with MitoTracker Red (red emission) for 30 min. As illustrated in Fig. 4A, cytochrome c is localised to the mitochondria in ρ^0 ASTC-a-1 cells (overlapping red and green pixels seen as yellow), there is no difference between the cytochrome c distribution in ASTC-a-1 and ρ^0 ASTC-a-1 cells. The release of cytochrome c was confirmed with the Western blotting analysis (Fig. 4B). Our data show that the quantity of released cytochrome c and the activation of the caspase-3 in ASTC-a-1 cells were significantly higher than in ρ^0 ASTC-a-1 cells after an identical PDT treatment (Fig. 4C and D).

3.6. Effect of endogenous ROS on cell apoptosis in Photofrin-PDT

To determine whether endogenous ROS contributed to cell apoptosis in Photofrin mediated PDT, we treated ASTC-a-1 and ρ^0 ASTC-a-1 cells with an identical PDT protocol (Photofrin 2.5 $\mu\text{g/ml}$ 3 J/cm^2). With confocal microscopy, it was shown that the DCF fluorescence intensity in ASTC-a-1 cells was significantly higher than that in the ρ^0 ASTC-a-1 cells after PDT (Fig. 5A). This is in concordance with that measured with FACS (Fig. 3C). When ASTC-a-1 and ρ^0 ASTC-a-1 cells were co-incubated with staurosporine (STS), there was no statistically significant difference in intracellular DCF fluorescence intensities between the two cell lines (Fig. 5B). This suggests that no endogenous ROS generation during apoptosis was induced by STS. The rate of apoptosis in ASTC-a-1 cells was significantly higher than ρ^0 ASTC-a-1 cells after identical dose PDT treatments, however, the rates of apoptosis induced by STS are not significantly different (Fig. 5C and D). These results suggest that endogenous ROS plays an important role in apoptosis induced by low dose PDT.

4. Discussion

Mitochondria are the major source of intracellular ROS during respiration. To determine whether the additional ROS was related to ETC, we established a mitochondrial respiration-deficient cell line (ρ^0 cells) (Fig. 2A). Given the same incubation

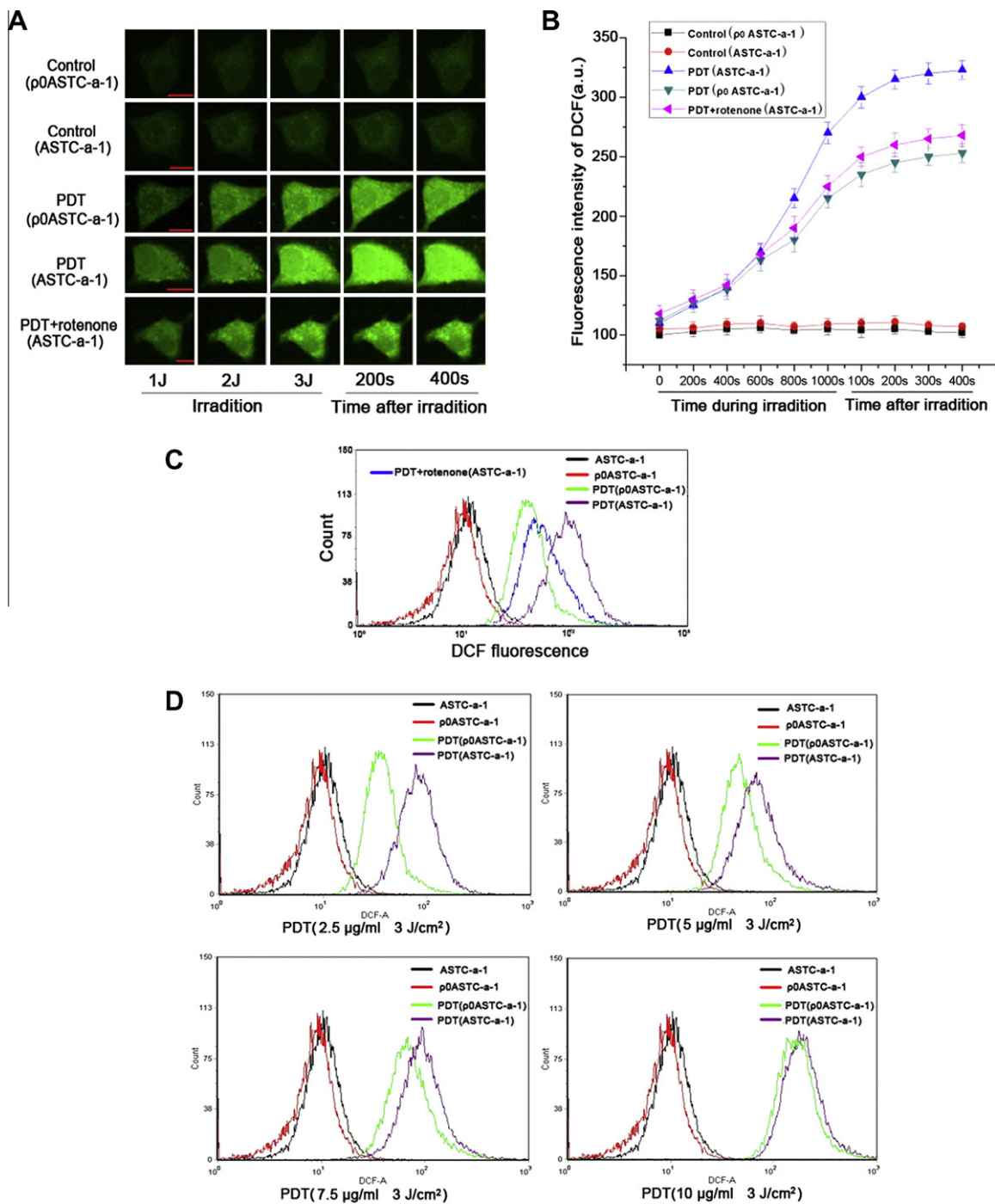


Fig. 3 – The difference of intracellular ROS generation between ASTC-a-1 and ρ^0 ASTC-a-1 cells with the identical dose PDT treatment. (A) Real-Time Detection of ROS generation during PDT (Photofrin 2.5 $\mu\text{g}/\text{ml}$ 3 J/cm^2) by a laser scanning confocal microscopy. Bar = 10 μm . (B) Quantitative analysis of relative DCF fluorescence intensity from cells treated by PDT or PDT in the presence of rotenone. Cells with no treatment were control. Data represent mean \pm SEM ($n = 5$). (C) FACS analysis of intracellular ROS generation of two cell lines after the identical dose PDT treatment. ASTC-a-1 cells were pretreated with the rotenone (2.5 μM) 30 min before PDT treatment. Untreated or treated cells were harvested and stained with 10 μM DCF for 30 min in the dark before being analysed by FACS. (D) The generation of intracellular ROS in both cell types with the increasing of Photofrin dose. (E) The difference in endogenous ROS between low (3 J/cm^2) and high dose (30 J/cm^2) PDT at a single Photofrin concentration (2.5 $\mu\text{g}/\text{ml}$). ROS generation was measured by DCF and analysed by FACS. (F) The difference of cell death with increasing Photofrin concentrations or light doses in both the wild type and the rho-zero cells. Cell death was analysed by FACS. Data represent mean \pm SEM ($n = 3$). (G) The analysis of cell death with increasing light doses at a high Photofrin concentration (10 $\mu\text{g}/\text{ml}$). Cell death was analysed by FACS. Data represent mean \pm SEM ($n = 3$).

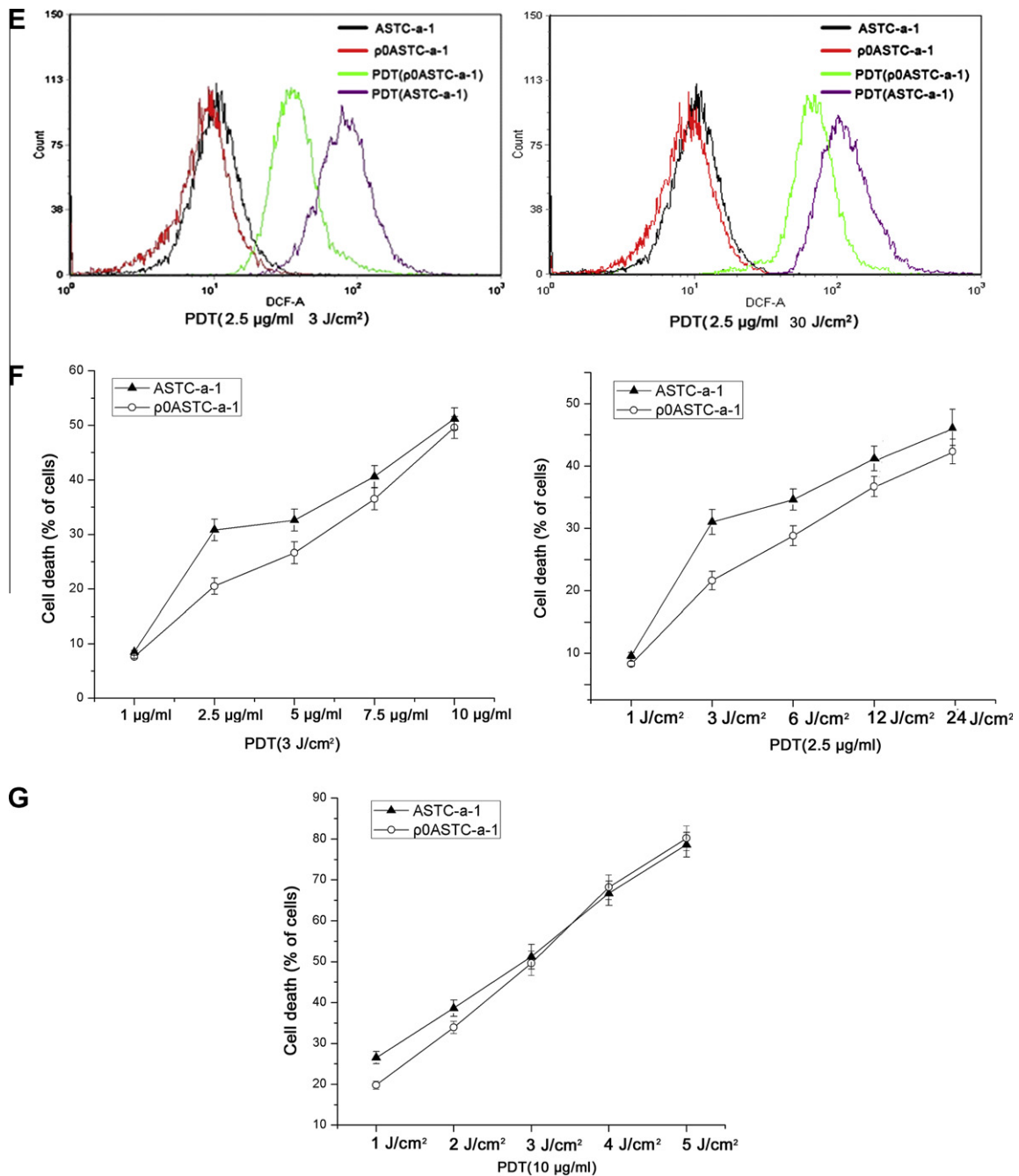


Fig 3. (continued)

and treatment protocols, there was no significant difference between the two cell lines in the final concentrations of photosensitiser present in cells (Fig. 2B). The spatial distribution of Photofrin in both cells was also similar (Fig. 2C). Previous studies have shown that loss of mtDNA does not alter cell cycle response.³² These results suggest that, p⁰ cells was a true negative control for intact cells to investigate whether endogenous ROS was from mitochondria during PDT.

Several studies have been reported in the literature, using the paired cell lines with the normal and deficient complement of mtDNA. The conclusions are not definitive. One study by Munday et al. used a mitochondria-localising boronated porphyrin (BOPP) in human Namalwa B lymphoma cells and

demonstrated resistance to PDT in mtDNA-depleted cells.³³ Keshav K. Singh agreed with this result.³² One study by Morgan, found that there was no differential phototoxicity between intact cells and mtDNA-depleted cells.²⁷ The mechanisms of p⁰ cells resistance to PDT are unknown. Our results show that the level of intracellular ROS in intact cells is higher than that in mtDNA-depleted cells after identical dose PDT treatment. The electron transport chain inhibitor rotenone significantly decreased intracellular ROS in intact cells (Fig. 3A and C). These results provide direct evidence that PDT induced endogenous ROS in mitochondria of intact cells. In the current study, it was observed that the rate of endogenous ROS generation depended on the Photofrin dose. With

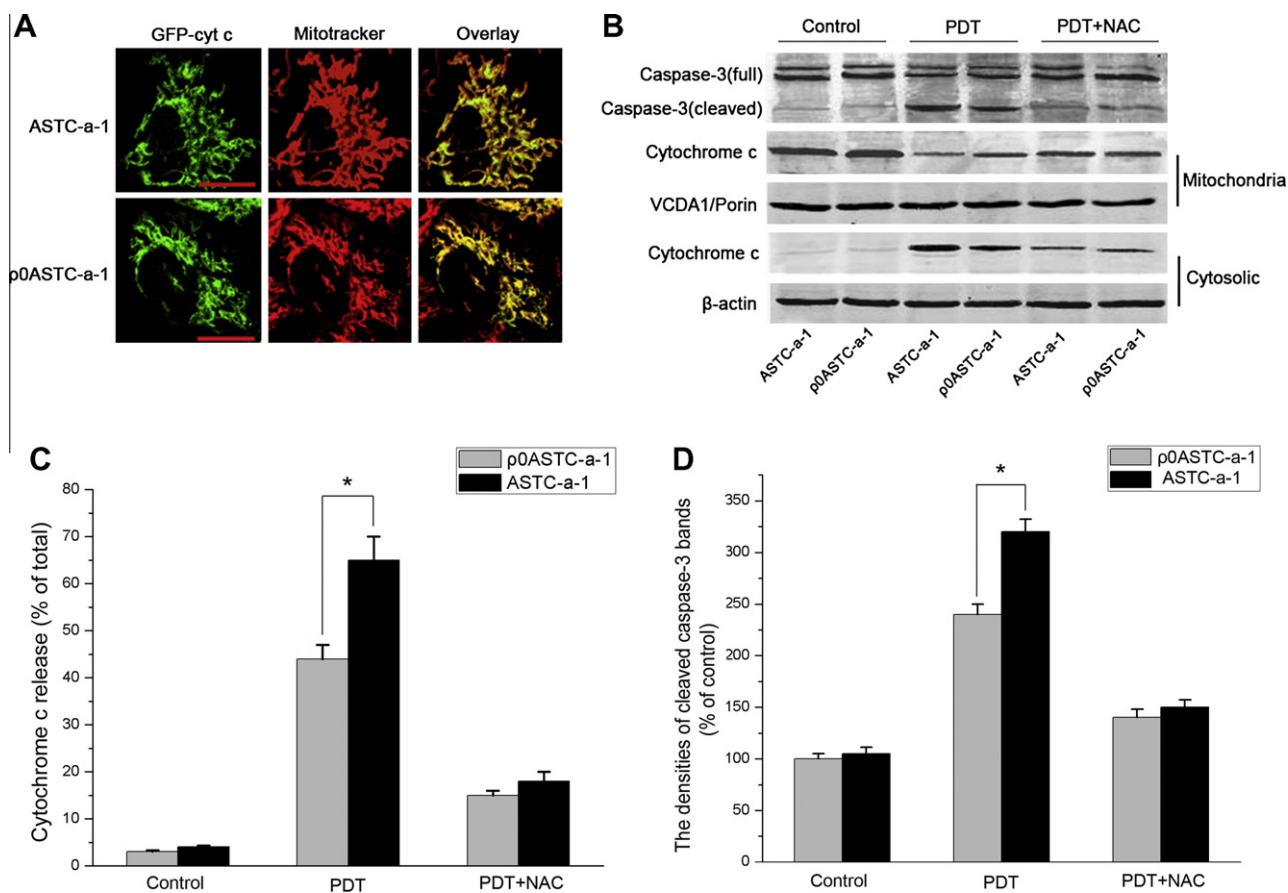


Fig. 4 – Western blotting analysis of proapoptotic proteins in both cells after an identical PDT treatment (Photofrin 2.5 $\mu\text{g}/\text{ml}$ 3 J/cm²). (A) ASTC-a-1 and p⁰ASTC-a-1 cells were transfected with pGFP-cyt c (green emission) and stained with MitoTracker Red (red emission) for 30 min. Overlay of the separate image shows that cytochrome c is localised to the mitochondria. Bar = 10 μm . (B) Immunoblot analysis of proapoptotic proteins (full caspase-3, cleaved caspase-3, and cytochrome c). (C) Quantification of cytochrome c release. Data represent mean \pm SEM ($n = 3$, $p < 0.05$). (D) The densities of cleaved caspase-3 bands were measured and the ratio was calculated and compared to the untreated cells. Data represent mean \pm SEM ($n = 3$, $p < 0.05$). (For interpretation of the references to colour in this figure legend, the reader is referred to the web version of this article.)

our investigated protocols, higher the Photofrin dose, lower the generation of endogenous ROS. When the Photofrin dose reached 10 $\mu\text{g}/\text{ml}$, the observed endogenous ROS was close to a complete abolition (Fig. 3D). It is thus suggested that, the previous conclusions that intracellular ROS is all from photosensitiser during PDT or there was no differential phototoxicity between intact cells and mtDNA-depleted cells might not be universal, as the selection of the treatment protocol can significantly affect the treatment outcome. It was previously shown that the prolonged, low-irradiance light delivery was more effective in tumour treatment and the mechanistic basis for the superiority of low-fluence rate PDT has been interpreted primarily as an improved tissue oxygenation. Our results show that, low dose PDT is able to induce more endogenous ROS that can directly improve the PDT toxicity.

ROS are products of aerobic metabolism. Results presented in this study draw a clear distinction between photoactive ROS that is generated directly from Photofrin mediated photochemical reactions and endogenous ROS that is from ETC (Fig. 3A and C). Notably, the production of endogenous ROS

during a low fluence rate PDT treatment started while the irradiation was being delivered (Fig. 3A and C).

Cytochrome c is a nuclear DNA-encoded protein. After being imported to mitochondria, cytochrome c resides in the space between the outer and inner membranes of mitochondria.³⁴ The release of cytochrome c was accompanied by the activation of DEVD-AMC cleavage activity.³⁵ Therefore, cytochrome c-mediated caspase activation is preserved in cells lacking mitochondrial function.³⁶ Jacobson et al. used p⁰ cells to investigate the role of mitochondria in apoptosis. They show that apoptosis can still occur in p⁰ cells and that over-expression of Bcl-2 can protect these cells from apoptosis.³⁷ Thus, despite the depletion of mtDNA and the absence of mitochondrial respiration, p⁰ cells can still undergo apoptosis and mitochondrial cytochrome c release, followed by caspase activation.³⁸ Our results show that, Photofrin mediated PDT caused cytochrome c release from mitochondria and NAC, a scavenger of ROS, attenuated the cytochrome c release (Fig. 4C). The release of cytochrome c and cell apoptosis are apparently different in the two cell lines after identical PDT

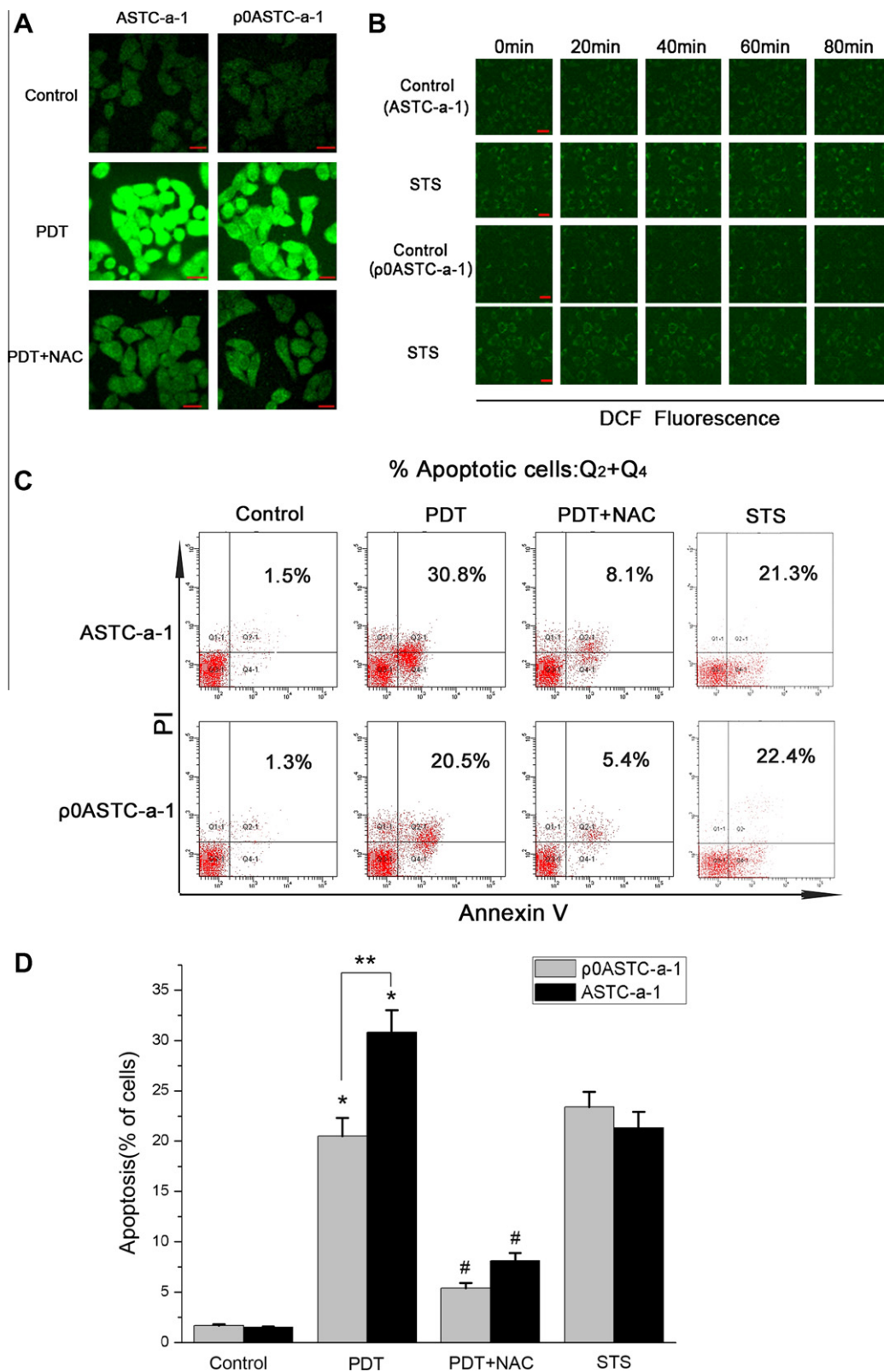


Fig. 5 – Effect of endogenous ROS on cell apoptosis in Photofrin-PDT. (A) The DCF fluorescence intensity in both cells was measured by laser confocal microscopy. ROS levels in cells treated with the antioxidant *N*-acetylcysteine (NAC; 2.5 mM) are shown for comparison. Bar = 20 μ m. **(B)** ASTC-a-1 and ρ^0 ASTC-a-1 cells were incubated with STS (5 μ M) in DMEM under 5% CO₂ at 37 °C and a fluorescence image of the cells was obtained by laser confocal microscopy. Much less or almost no fluorescence was observed for both cell line. Bar = 20 μ m. **(C)** Analysis of PDT/STS-induced apoptosis of two cell lines, cells were stained with FITC-conjugated Annexin V and propidium iodide. **(D)** The percentage of apoptosis cells were used to calculate. Data represent mean \pm SEM ($n = 4$, * $p < 0.05$, compared with control; # $p < 0.05$, compared with PDT treatment; ** $p < 0.01$).

protocol. The rate of apoptosis in ASTC-a-1 cells (with functioning mitochondria enabling to generate endogenous ROS) is significantly higher than that with the ρ^0 ASTC-a-1 cells (with the mitochondrial respiration abrogated). ROS scavenger NAC attenuated the toxicity of PDT in both cell lines (Fig. 5C). It indicates that endogenous ROS may contribute to the cytochrome c release and cell apoptosis in the PDT treatment.

Staurosporine is one of the most commonly used agents to experimentally induce cell apoptosis. Apoptosis occurs in essentially all cell types when they are exposed to appropriate concentrations of staurosporine.^{39,40} Our results show that, mitochondrial respiration did not generate ROS during apoptosis induced by staurosporine in ρ^0 cells and intact cells (Fig. 5B). There is no significant difference in apoptosis induced by staurosporine between ρ^0 cells and intact cells (Fig. 5D). These data further indicate that the difference of apoptosis induced by PDT is dependent on the generation of endogenous ROS in intact cells.

In conclusion, our data show that the extent of the PDT-induced endogenous ROS depends on the dose of PDT. Low dose PDT is more effective in induction of endogenous ROS via the ETC. This endogenous ROS contributes to an increased cell apoptosis. This study may help us further our understanding that a low-fluence rate PDT is more effective in tumour treatment. The current research provides an insight of cellular apoptosis mechanism for those cells exposed to low dose PDT. This is especially important for the treatment of cells located in the centre of tumours where the optical attenuation of the tissue could reduce the irradiation light fluence to very low levels. Moreover, the results of the current study may help improving clinical application by maximising the efficiency of currently available photosensitisers.

Conflict of interest statement

None declared.

Acknowledgements

This research is supported by the National Basic Research Program of China (2011CB910402, 2010CB732602), the Program for Changjiang Scholars and Innovative Research Team in University (IRT0829), and the National Natural Science Foundation of China (30870676, 30870658). We thank Dr. G.J. Gores (Center for Basic Research in Digestive Diseases, Molecular Medicine Program, Mayo Clinic, Rochester Minnesota) for kindly providing the pGFP-cyt c.

REFERENCES

- Dougherty TJ, Marcus SL. Photodynamic therapy. *Eur J Cancer* 1992;10:1734–42.
- Seshadri M, Bellnier DA, Vaughan LA, et al. Light delivery over extended time periods enhances the effectiveness of photodynamic therapy. *Clin Cancer Res* 2008;14:2796–805.
- Mathews MS, Angell-Petersen E, Sanchez R, et al. The effects of ultra low fluence rate single and repetitive photodynamic therapy on glioma spheroids. *Lasers Surg Med* 2009;41:578–84.
- Weishaupt KR, Gomer CJ, Dougherty TJ. Identification of singlet oxygen as the cytotoxic agent in photoinactivation of a murine tumor. *Cancer Res* 1976;36:2326–9.
- Chen B, Roskams T, Xu Y, Agostinis P, de Witte PA. Photodynamic therapy with hypericin induces vascular damage and apoptosis in the RIF-1 mouse tumor model. *Int J Cancer* 2002;98:284–90.
- Kessel D, Luo Y. Mitochondrial photodamage and PDT-induced apoptosis. *J Photochem Photobiol B* 1998;42:89–95.
- Kessel D, Luo Y, Deng Y, Chang CK. The role of subcellular localization in initiation of apoptosis by photodynamic therapy. *Photochem Photobiol* 1997;65:422–6.
- Salet C, Moreno G, Ricchelli F, Bernardi P. Singlet oxygen produced by photodynamic action causes inactivation of the mitochondrial permeability transition pore. *J Biol Chem* 1997;272:21938–43.
- Oleinick NL, Evans HH. The photobiology of photodynamic therapy: cellular targets and mechanisms. *Radiat Res* 1998;150:S146–56.
- Lam M, Oleinick NL, Nieminen AL. Photodynamic therapy-induced apoptosis in epidermoid carcinoma cells. Reactive oxygen species and mitochondrial inner membrane permeabilization. *J Biol Chem* 2001;276:47379–86.
- Wallace DC. Mitochondrial diseases in man and mouse. *Science* 1999;283:1482–8.
- Chance B, Sies H, Boveris A. Hydroperoxide metabolism in mammalian organs. *Physiol Rev* 1979;59:527–605.
- Campian JL, Qian M, Gao X, Eaton JW. Oxygen tolerance and coupling of mitochondrial electron transport. *J Biol Chem* 2004;279:46580–7.
- Campian JL, Gao X, Qian M, Eaton JW. Cytochrome C oxidase activity and oxygen tolerance. *J Biol Chem* 2007;282:12430–8.
- Wu S, Xing D, Wang F, Chen T, Chen WR. Mechanistic study of apoptosis induced by high-fluence low-power laser irradiation using fluorescence imaging techniques. *J Biomed Opt* 2007;12:064015.
- Becker LB. New concepts in reactive oxygen species and cardiovascular reperfusion physiology. *Cardiovasc Res* 2004;61:461–70.
- Harman D. The free radical theory of aging. *Antioxid Redox Signal* 2003;5:557–61.
- Barrientos A, Moraes CT. Titrating the effects of mitochondrial complex I impairment in the cell physiology. *J Biol Chem* 1999;274:16188–97.
- Chen Q, Vazquez EJ, Moghaddas S, Hoppel CL, Lesnefsky EJ. Production of reactive oxygen species by mitochondria: central role of complex III. *J Biol Chem* 2003;278:36027–31.
- Schatz G. Mitochondria: beyond oxidative phosphorylation. *Biochim Biophys Acta* 1995;1271:123–6.
- King MP, Attardi G. Human cells lacking mtDNA: repopulation with exogenous mitochondria by complementation. *Science* 1989;246:500–3.
- King MP, Attardi G. Injection of mitochondria into human cells leads to a rapid replacement of the endogenous mitochondrial DNA. *Cell* 1988;52:811–9.
- Wang W, Fang H, Groom L, et al. Superoxide flashes in single mitochondria. *Cell* 2008;134:279–90.
- Zuckerbraun BS, Chin BY, Bilban M, et al. Carbon monoxide signals via inhibition of cytochrome c oxidase and generation of mitochondrial reactive oxygen species. *FASEB J* 2007;21:1099–106.
- Brunelle JK, Shroff EH, Perlman H, et al. Loss of Mcl-1 protein and inhibition of electron transport chain together induce anoxic cell death. *Mol Cell Biol* 2007;27:1222–35.

26. King MP, Attardi G. Isolation of human cell lines lacking mitochondrial DNA. *Methods Enzymol* 1996;**264**:304–13.
27. Morgan J, Potter WR, Oseroff AR. Comparison of photodynamic targets in a carcinoma cell line and its mitochondrial DNA-deficient derivative. *Photochem Photobiol* 2000;**71**:747–57.
28. Doerries C, Grote K, Hilfiker-Kleiner D, et al. Critical role of the NAD(P)H oxidase subunit p47phox for left ventricular remodeling/dysfunction and survival after myocardial infarction. *Circ Res* 2007;**100**:894–903.
29. Athar M, Elmets CA, Bickers DR, Mukhtar H. A novel mechanism for the generation of superoxide anions in hematoporphyrin derivative-mediated cutaneous photosensitization. Activation of the xanthine oxidase pathway. *J Clin Invest* 1989;**83**:1137–43.
30. Turrens JF. Mitochondrial formation of reactive oxygen species. *J Physiol* 2003;**552**:335–44.
31. Turrens JF. Superoxide production by the mitochondrial respiratory chain. *Biosci Rep* 1997;**17**:3–8.
32. Singh KK, Russell J, Sigala B, et al. Mitochondrial DNA determines the cellular response to cancer therapeutic agents. *Oncogene* 1999;**18**:6641–6.
33. Munday AD, Sriratana A, Hill JS, Kahl SB, Nagley P. Mitochondria are the functional intracellular target for a photosensitizing boronated porphyrin. *Biochim Biophys Acta* 1996;**1311**:1–4.
34. Stuart RA, Neupert W. Apocytochrome c: an exceptional mitochondrial precursor protein using an exceptional import pathway. *Biochimie* 1990;**72**:115–21.
35. Liu X, Kim CN, Yang J, Jemmerson R, Wang X. Induction of apoptotic program in cell-free extracts: requirement for dATP and cytochrome c. *Cell* 1996;**86**:147–57.
36. Jiang S, Cai J, Wallace DC, Jones DP. Cytochrome c-mediated apoptosis in cells lacking mitochondrial DNA signaling pathway involving release and caspase 3 activation is conserved. *J Biol Chem* 1999;**274**:29905–11.
37. Jacobson MD, Burne JF, King MP, et al. Bcl-2 blocks apoptosis in cells lacking mitochondrial DNA. *Nature* 1993;**361**:365–9.
38. Marchetti P, Susin SA, Decaudin D, et al. Apoptosis-associated derangement of mitochondrial function in cells lacking mitochondrial DNA. *Cancer Res* 1996;**56**:2033–8.
39. Tsuruta F, Masuyama N, Gotoh Y. The phosphatidylinositol 3-kinase (PI3K)-Akt pathway suppresses Bax translocation to mitochondria. *J Biol Chem* 2002;**277**:14040–7.
40. Zhang L, Zhang Y, Xing D. LPLI inhibits apoptosis upstream of Bax translocation via a GSK-3beta-inactivation mechanism. *J Cell Physiol* 2010;**224**:218–28.